International Journal of Automotive Technology, Vol. 7, No. 3, pp. 337–343 (2006)

1229–9138/2006/027–15

CORRELATION BETWEEN J-INTEGRAL AND CMOD IN IMPACT BEHAVIOR OF 3-POINT BEND SPECIMEN

M. S. HAN[1)*] and J. U. CHO[2)]

[1)]School of Mechanical and Automotive Engineering, Keimyung University, Daegu 704-701, Korea
[2)]Faculty of Mechanical and Automotive Engineering, Gongju National University, Chungnam 330-717, Korea

(Received 26 October 2005; Revised 9 December 2005)

ABSTRACT–Numerical calculations are made in order to find a possible correlation between the J-integral and the crack mouth opening displacement (CMOD) in dynamic nonlinear fracture experiments of 3-point bend (3PB) specimens. Both elastic-plastic and elastic-viscoplastic materials are considered at different impact velocities. The J-integral may be estimated from the crack mouth opening displacement which can be measured directly from photographs taken during dynamic experiments.

KEY WORDS : Dynamic nonlinear fracture, 3PB specimen, Crack mouth opening displacement, Viscoplastic property, J-integral

1. INTRODUCTION

During the development of dynamic fracture mechanics, many investigations have been made on the dynamic behavior of the impact loaded 3PB specimen and the influence of the boundary conditions at the impact points (Van Elst, 1984; Bergmark and Kao, 1991). Nowadays, the dynamic analysis is also applied to the area of automobile (Jang and Chae, 2000; Cheon and Meguid, 2004). The J-integral used as a ductile crack initiation criterion has been discussed for the dynamically loaded elastic-plastic 3PB specimens (Zehnder *et al.*, 1990; Nakamura *et al.*, 1986). Some experimental methods to measure or estimate the J-integral history have been investigated and compared to the theoretically obtained values. For example, a caustic method has been successfully applied (Zehnder *et al.*, 1990). Another method is to use the multiple strain gauge measurements and then to estimate the J-integral value near the crack tip (Nakamura *et al.*, 1986). It is well known that a correlation between the J-integral and CMOD exists under the static and small scale yielding condition (Shih, 1982). In this paper, numerical calculations are performed in order to find a correlation between the J-integral and CMOD for the dynamic nonlinear stationary crack. And then, the dynamical J-integral history has been estimated at different impact velocities (V_0 = 15, 30, 45, 60 m/s) from the correlation between CMOD and J-integral. Both elastic-plastic and elastic-viscoplastic materials are considered. Numerical simulations are made by using the FEM code, ABAQUS (2003). These results can be utilized in the basic design in the impact analysis of automobile. The purpose of this study is to evaluate the safety parameter of the nonlinear plastic specimen by impact.

*Corresponding author. e-mail: sheffhan@kmu.ac.kr

2. FINITE ELEMENT MODEL

The geometry and the finite element model of the specimen are shown in Figure 1 and Figure 2 respectively. The dimensions of this specimen are given as shown in Figure 2.

Due to the symmetry, only half a specimen is modeled. A two-dimensional mesh including 92 eight node plane stress elements with 2×2 Gauss points, i.e. with reduced integration, is chosen. The mesh near the crack tip is concentrated by using the degenerated eight node ele-

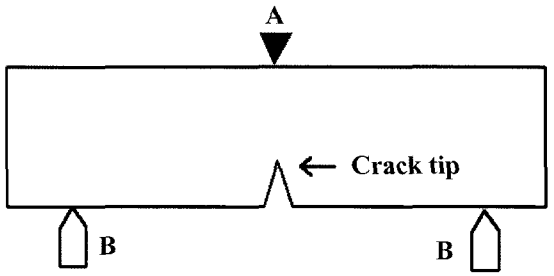

Figure 1. Geometry of the specimen.

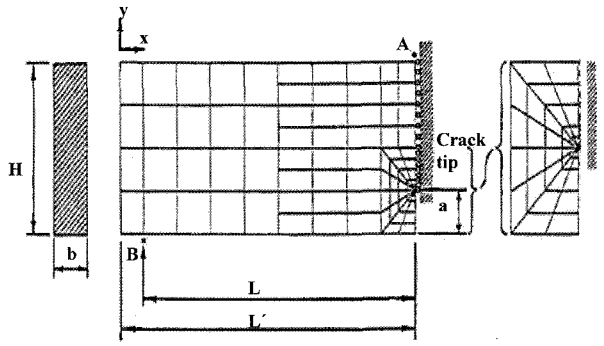

Figure 2. Finite element model for 3PB specimen with a quarter notch (L=300 mm, L'=320 mm, H=75 mm, b=18 mm, a=H/4=18.75 mm).

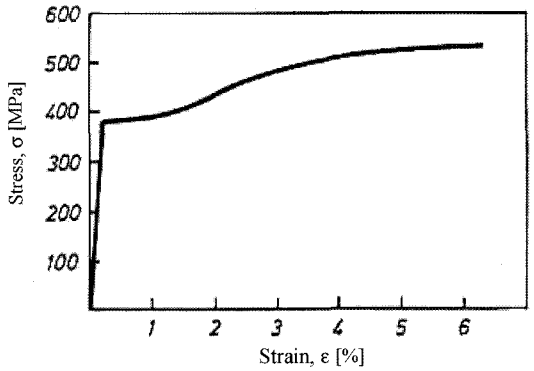

Figure 3. Static tensile test diagram.

ments. In order to model a possible loss of contact at the load point A and at the support points B which had been discussed (Bergmark and Kao, 1991), gap elements with one degree of freedom are introduced. Furthermore, a lumped mass element is used to model the impact head in Figure 2. No crack propagation is taken into account in the calculations. The dynamical J-integral and CMOD are calculated using the commercial finite element method code, ABAQUS (2003). In this code, the virtual crack extension method is successfully used to evaluate the J-integral in the dynamic case (Nakamura *et al.*, 1985). The experiment of cited paper (Bergmark and Kao, 1991) is run at impact velocity of 45 m/s to inspect this simulation model in this study. The dynamically loaded 3-point bending ductile steel specimens are made to compare with numerical simulation.

The geometry and dimensions of this specimen are same to the one in Figure 1 and Figure 2. This material is Mn-alloyed normalized steel. The result of tensile test is shown in Figure 3. The experimental display (Bergmark and Kao, 1991) is also shown in Figure 4. The U-shaped hammer is accelerated to a prescribed velocity and hits the 3PB specimen at the side points B as shown in Figure 1. This specimen is supported at the middle point A. Two

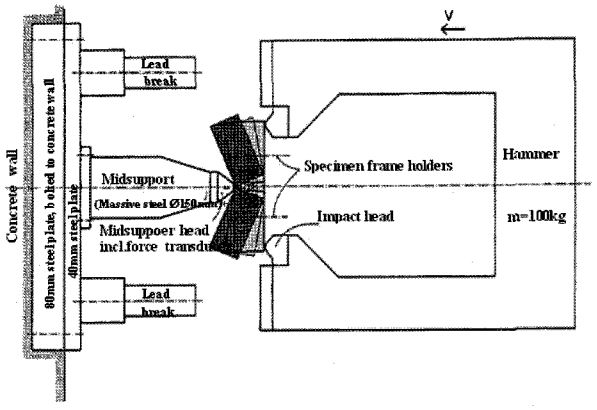

Figure 4. Cited experimental display.

hardened and tempered impact heads with cylindrical contact surfaces are attached to the hammer. The recordings during the experiments include high speed photography, mid support force measurements and impact detection. Plane stress in FEM simulation is made under the assumption of no crack growth. The material of this specimen is treated as an elastic-plastic material using an isotropic hardening von Mises model, i.e., the possible effects of rate dependent material properties are ignored. The used mesh is same to Figure 2 in this study. The side points B of the specimen are impacted by a U-shaped hammer. Due to the bending of the specimen, the friction forces parallel with the specimen surface may be introduced during impact. To investigate this aspect, two different boundary conditions at the impact points are considered in two simulations: roller and locking. The mid-support forces obtained from the experiments and the simulations are presented in Figure 5 for the impact velocity of 45 m/s. It is notable that the experiments give

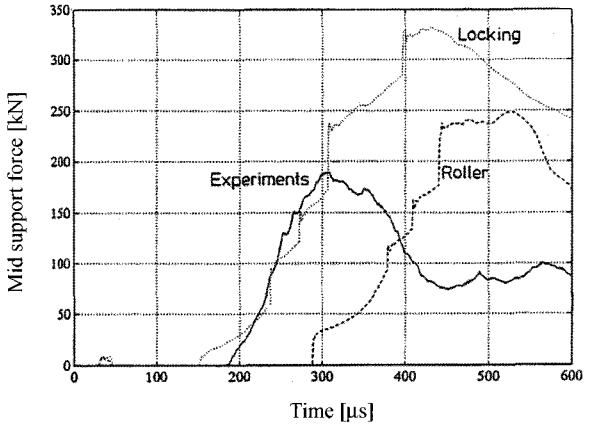

Figure 5. Mid-support force versus time at the impact velocity of 45 m/s for the two different simulations and the experiment (experiment: solid line, simulations, roller boundary: broken line, locking boundary: dotted line).

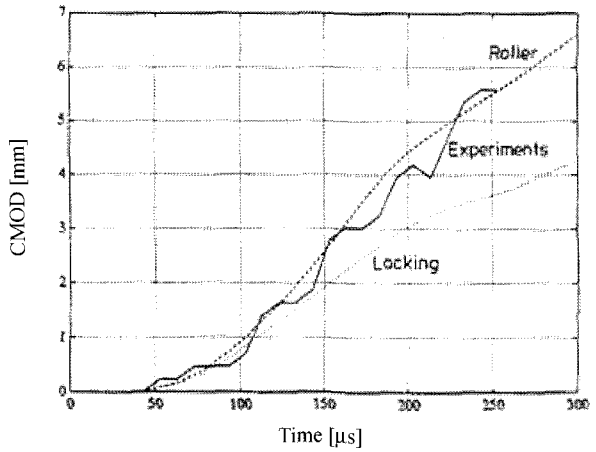

Figure 6. CMOD versus time at the impact velocity of 45 m/s for the two different simulations and the experiment (experiment: solid line, simulations, roller boundary: broken line, locking boundary: dotted line).

the results which become closer to the numerical simulation with the locking boundary condition than with the roller boundary condition. The CMOD simulations for both sets of the boundary conditions are also shown in Figure 6 for the impact velocity of 45 m/s together with the experimentally found values. The experiments for CMOD curves become between the numerical simulations with locking boundary and with the roller boundary condition as shown in Figure 6.

Therefore, the inspection of this specimen model in this presented paper is sufficient for the numerical simulation. The numerical simulations are made with locking boundary condition in this paper.

3. RESULTS FROM ELASTIC-PLASTIC ANALYSIS WITH 3 PB SPECIMEN

An isotropic elastic-plastic hardening von Mises material is modeled with Young's modulus E=206 GPa, Poisson's ratio υ=0.3, Density Φ=7800 kg/m^3 and yielding stress σ_Y=360 MPa. The static stress to strain curve is shown in Figure 7.

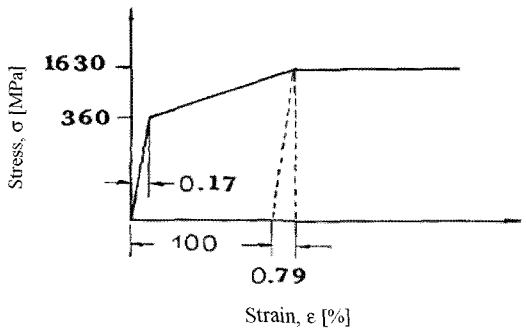

Figure 7. Static stress-strain curve of the material.

The specimen in this study is loaded at the middle point A by an impact head with a weight of 1.96 kN. Four different impact velocities are chosen for the simulations. These calculations are run up to 600 μs after impact. The correlation between the J-integral and the crack tip opening displacement (CTOD or δ_t) in Barenblatt's model (Kanninen and Popelar, 1985) can be formulated as:

$$J = \int_0^{\delta_t} \sigma(\delta) d\delta \tag{1}$$

For the Dugdale model (Kanninen and Popelar, 1985), the following equation holds as:

$$J = \delta_t \sigma_Y \tag{2}$$

In case of elastic-plastic material and small-scale yielding condition, finite element calculations (Knott, 1973) are given as follows:

$$J = \alpha \delta_t \sigma_Y \tag{3}$$

where α has been found to be in the range 1.0–1.7 in plane stress cases (Knott, 1973). Shih (1982) finds that in case of power law hardening, the parameter α depends primarily upon the strain hardening exponent n.

The relation between δ_t and δ_M in the elastic-plastic 3PB specimen (Broek, 1982) can be shown in Figure 8 as follows:

$$\delta_t = \frac{\delta_M}{1 + \dfrac{a}{r(H-a)}} = \gamma \delta_M \tag{4}$$

Thus, assuming that the plastic hinge in Figure 8 does not move before crack growth, we obtain as:

$$J = \alpha \delta_t \sigma_Y \text{ or } J = \beta \delta_M \sigma_Y \tag{5}$$

with $\beta = \alpha_Y$

The J-integral and CMOD history can also be found at every time step. And then, it is found that the correlation between J=$J(V_o,t)$ and CMOD=$\delta_M(V_o,t)$ can be written as:

$$J(V_o,t) = \beta(V_o)\sigma_Y \delta_M(V_o,t) \tag{6}$$

where $\beta(V_o)$ is estimated by the least square method.

With k being the number of time increments in the

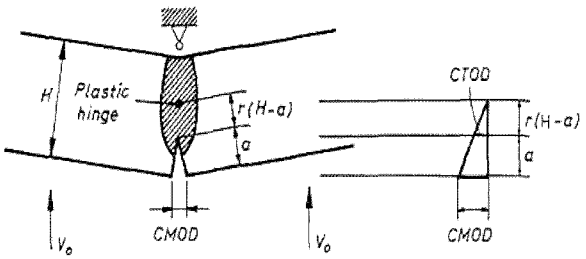

Figure 8. Plastic hinge, CTOD and CMOD.

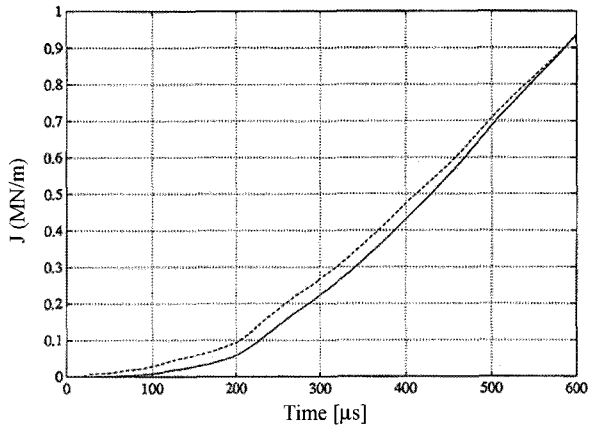

Figure 9. J-integral (solid line) and $\beta(V_o)\sigma_Y\delta_M$ (dashed line) history at the impact velocity of 15 m/s. (β is chosen as 0.76) in case of elastic-plastic material.

finite element calculations, we obtain as:

$$\beta(V_o) = \frac{\sum_{i=1}^{k} J(V_o)\delta_{Mi}(V_o)}{\sigma_Y \sum_{i=1}^{k} \delta_{Mi}(V_o)^2} \tag{7}$$

where J_i and δ_{Mi} are the calculated values of J and δ_M at time i.

The following $\beta(V_o)$ values are found as:

$$\beta(15)=0.72 \quad \beta(30)=0.78 \qquad (8)$$
$$\beta(45)=0.79 \quad \beta(60)=0.76$$

These results suggest that $\beta(V_o)$ is insensitive to the impact velocity V_o and so, we may take $\beta=\beta(V_o)=0.76$, i.e. the mean value of the above results.

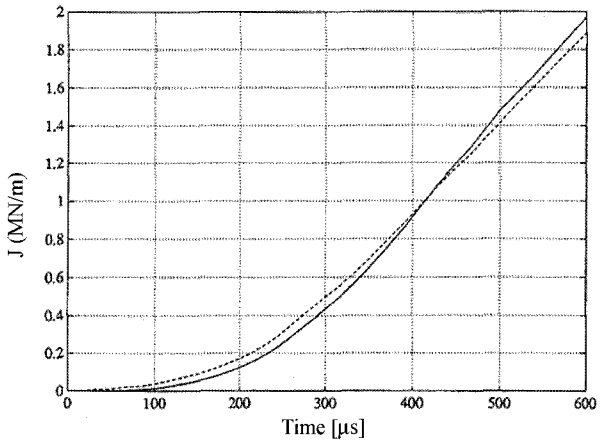

Figure 10. J-integral (solid line) and $\beta(V_o)\sigma_Y\delta_M$ (dashed line) history at the impact velocity of 30 m/s. (β is chosen as 0.76) in case of elastic-plastic material.

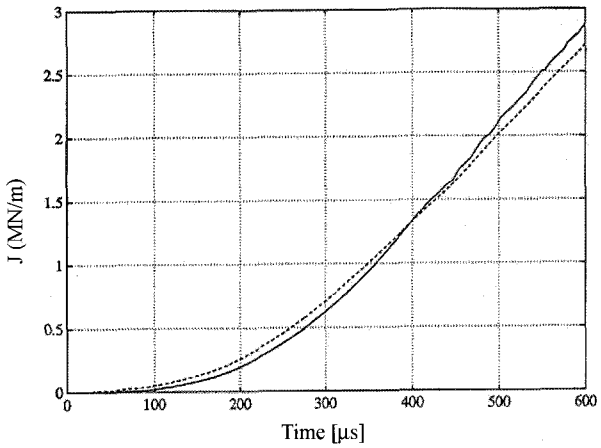

Figure 11. J-integral(solid line) and $\beta(V_o)\sigma_Y\delta_M$ (dashed line) history at the impact velocity of 45 m/s. (β is chosen as 0.76) in case of elastic-plastic material.

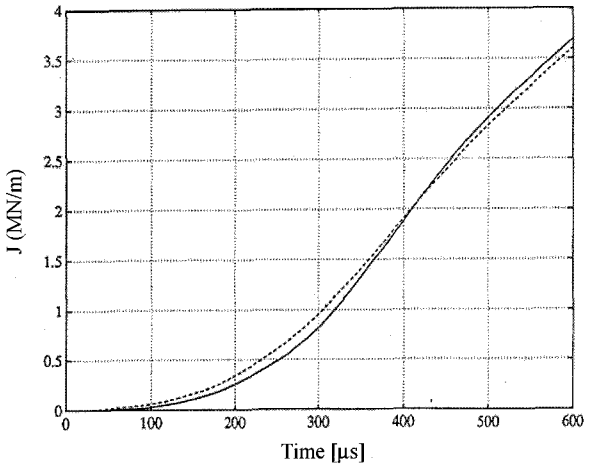

Figure 12. J-integral (solid line) and $\beta(V_o)\sigma_Y\delta_M$ (dashed line) history at the impact velocity of 60 m/s. (β is chosen as 0.76) in case of elastic-plastic material.

Indeed, the maximum error using this β-value is less than 5% when compared that using of β-values given by (8). Figures 9–12 show the J-integral and $\beta\cdot\sigma_Y$-CMOD history at the four different impact velocities of 15, 30, 45, and 60 m/s with β=0.76 in case of elastic-plastic material.

It can be shown that the value of J-integral becomes higher than that of $\beta\cdot\sigma_Y$-CMOD history at more than time of 400 μs after impact in Figures 10–12. As the impact velocity increases, the stress around crack tip increases. The value of J-integral becomes higher and so, this value tends to become higher than that of $\beta\cdot\sigma_Y$-CMOD history.

In Figures 9–12, the J-integral and $\beta\cdot\sigma_Y$-CMOD history are found to be in a good agreement. It is found that the parameter $\beta(V_o)$ is independent on any impact

velocity Vo in the studied range of impact velocity. By this result, as soon as the CMOD history, $\delta_M(V_o,t)$ is measured from experiments at a specific impact velocity in case of elastic-plastic material, the J-integral can be calculated according to the relation $J(V_o,t)=\beta(V_o)\cdot\sigma_Y\cdot\delta_M(V_o,t)$.

4. RESULTS FROM ELASTIC-VISCOPLASTIC ANALYSIS WITH 3 PB SPECIMEN

Since the impact velocities considered above are rather high, the rate dependent properties might have a marked effect. In order to investigate these phenomena, the viscoplastic behavior is introduced in this model. To provide a short exposition of this theory, we shall consider small strains for the moment.

In this case, the total strain rate $\dot{\varepsilon}_{ij}$ (Perzyna, 1966) is as follows:

$$\dot{\varepsilon}_{ij}=\dot{\varepsilon}^{e}_{ij}+\dot{\varepsilon}^{vp}_{ij} \tag{9}$$

where $\dot{\varepsilon}^{e}_{ij}$ is linearly related to the stress rate according to Hooke's law:

$$\dot{\varepsilon}^{e}_{ij}=\frac{1}{2\mu}\dot{s}_{ij}+\frac{1-2\upsilon}{E}\dot{s}\,\delta_{ij} \tag{10}$$

with $\dot{s}_{ij}=\dot{\sigma}_{ij}-\dot{s}\,\delta_{ij}$, $\dot{s}=\frac{1}{3}\dot{\sigma}_{ij}$

δ_{ij}=Kronecker's delta and μ=shear modulus

$\dot{\varepsilon}^{vp}_{ij}$ represents the combined viscous and plastic effects:

$$\dot{\varepsilon}^{vp}_{ij}=\gamma\Phi(F)\frac{\partial f}{\partial\sigma_{ij}} \tag{11}$$

where,

$$F=\frac{f(\sigma_{ij})}{\kappa}-1 \tag{12}$$

and

$$\Phi(F)=\begin{cases}0 & \text{If } F\le 0\\ \Phi(F) & \text{If } F>0\end{cases} \tag{13}$$

In the above equations, γ is a viscosity constant of the material and κ is a strain hardening parameter. f is the potential function that depends on the state of stress σ_{ij} for an isotropic work-hardening material. F is the yielding function and Φ is a function of F. All these quantities may be determined from the tests of material under dynamic loading.

When the von Mises yielding condition is assumed, the one dimensional form of (11) becomes as follows (Malvern, 1951):

$$\dot{\varepsilon}^{vp}=(2/\sqrt{3})\gamma\Phi\left(\frac{\sigma}{\sigma_Y}-1\right) \tag{14}$$

where σ_Y is the current yielding stress. By introducing $\Phi(F)=F^p$, we obtain as:

$$\dot{\varepsilon}^{vp}=D\left(\frac{\sigma}{\sigma_Y}-1\right)^{p} \tag{15}$$

where, $D=(2/\sqrt{3})\gamma$

In the calculations, the data of Brickstad (1983) are adopted, i.e. D=4100 1/s and p=2.

For the four impact velocities, the development with time of J-integral and CMOD-value is calculated. Then, the relation (6) between $J=J(V_o,t)$ is adopted.

Figures 13–16 show the J-integral and $\beta\cdot\sigma_Y$·CMOD history at the four impact velocities of 15, 30, 45 and 60 m/s with the viscoplasticity. In these cases, β varies according to the different impact velocities.

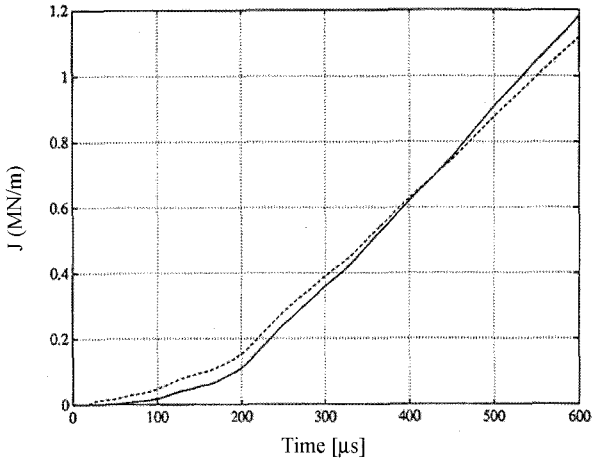

Figure 13. J-integral (solid line) and $\beta(V_o)\sigma_Y\delta_M$ (dashed line) history at the impact velocity of 15 m/s. (β is chosen as 0.85) in case of elastic-viscoplastic material.

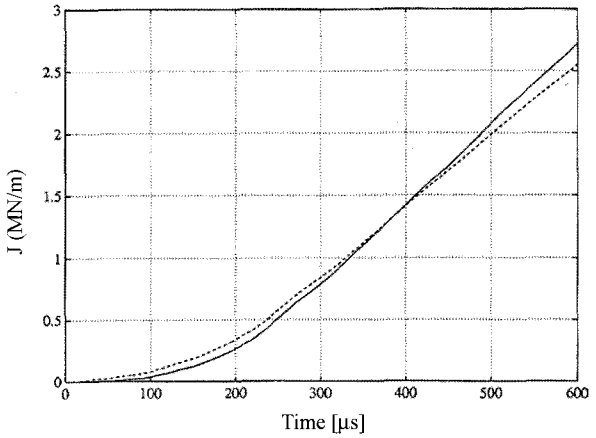

Figure 14. J-integral (solid line) and $\beta(V_o)\sigma_Y\delta_M$ (dashed line) history at the impact velocity of 30 m/s. (β is chosen as 0.94) in case of elastic-viscoplastic material.

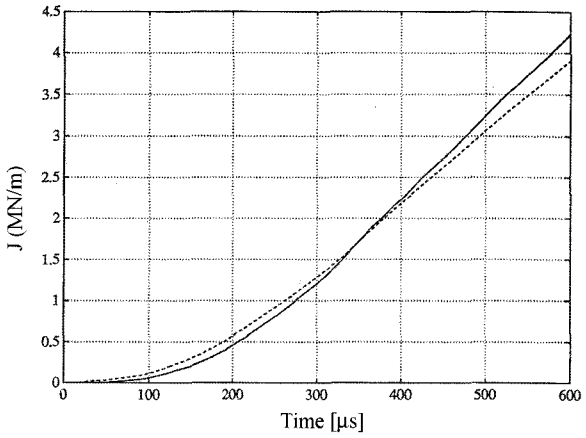

Figure 15. J-integral (solid line) and $\beta(V_o)\sigma_Y\delta_M$ (dashed line) history at the impact velocity of 45 m/s. (β is chosen as 0.98) in case of elastic-viscoplastic material.

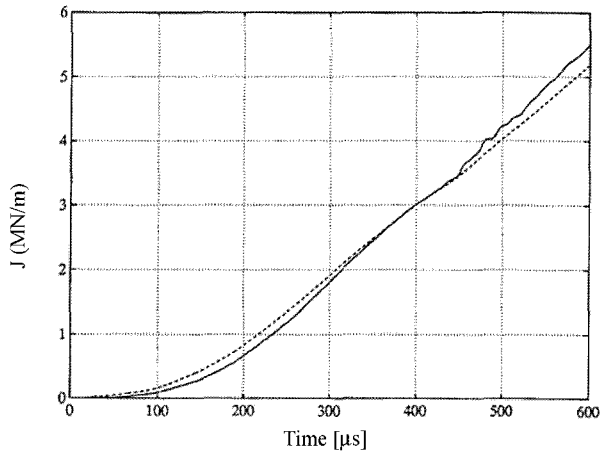

Figure 16. J-integral (solid line) and $\beta(V_o)\sigma_Y\delta_M$ (dashed line) history at the impact velocity of 60 m/s. (β is chosen as 1.03) in case of elastic-viscoplastic material.

Using (7) we obtain as:

$$\beta(15)=0.85 \quad \beta(30)=0.94 \quad \beta(45)=0.98 \quad \beta(60)=1.03 \tag{16}$$

It can be shown that the value of J-integral becomes higher than that of $\beta\cdot\sigma_Y$·CMOD history at more than time of 400 ms after impact in Figures 13–16. As the impact velocity increases, the stress around crack tip increases. The value of J-integral becomes higher and so, this value tends to become higher than that of $\beta\cdot\sigma_Y$·CMOD history. In Figures 13–16, the J-integral and $\beta\cdot\sigma_Y$·CMOD history are found to indicate a good agreement. From the β-values given by (16), a β-V_o curve as shown in Figure 17 can be established. The coefficient $\beta(V_o)$ varies according to the different impact velocities.

However, as $\beta(V_o)$ is determined at any impact velocity, the value of the J-integral for any impact velocity V_o can be guessed from CMOD experiments with this curve and the relation (6).

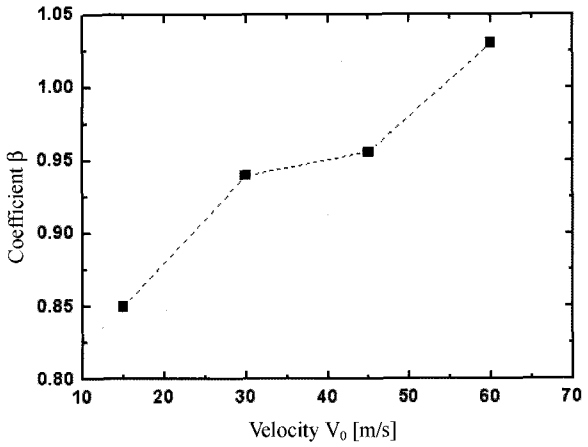

Figure 17. Estimated β-V_o curve for the viscoplastic model.

5. CONCLUSIONS

From the impact analysis for the nonlinear plastic behavior with the dynamically loaded 3PB specimens, the following results are obtained.

(1) The possibility relating the J-integral and the crack mouth opening displacement at the dynamically loaded 3PB specimens has been investigated. The J-integral can be the yielding stress multiplied by crack mouth opening displacement times $\beta(V_o)$.

(2) In the calculations of this study, the impact velocities are varied from 15 m/s up to 60 m/s. Two different material properties, i.e. elastic-plastic and elastic-viscoplastic properties have been considered.

(3) In case of elastic-plastic material, it is found that the parameter $\beta(V_o)$ is independent on any impact velocity V_o in the studied range of impact velocity. Thus, once β is determined by a finite element calculation for a specific material and geometry, the J-integral can be calculated from CMOD experiments.

(4) For an elastic-viscoplastic material, a linear correlation between the J-integral and the crack mouth opening displacement is found. The coefficient $\beta(V_o)$ varies according to different impact velocities. However, as $\beta(V_o)$ is determined at any impact velocity, the value of the J-integral can be guessed from CMOD experiments.

REFERENCES

ABAQUS Manual (2003). *Version 6.4, Karlsson and*

Sorensen Inc. Pawtucket. U.S.A.

Bergmark, A. and Kao, H. R. (1991). Dynamic crack initiation in 3PB ductile steel specimens. *Technical Report. LUTFD2 TFHF-3041, Lund Institute of Technology*, Sweden, 1–23.

Brickstad, B. (1983). Viscoplastic analysis of rapid crack propagation experiments in steel. *Mech. Phys. Solids* **31, 4,** 307–332.

Broek, D. (1982). *Elementary Engineering Fracture Mechanics*. 3rd Edn., Martinus Nijhoff Publishers. The Netherlands.

Cheon, S. S. and Meguid, S. A. (2004). Crush behavior of metallic foams for passenger car design. *Int. J. Automotive Technology* **5, 1,** 47–53.

Jang, I. S. and Chae, D. B. (2000). The derivation of simplified vehicle body stiffness equation using collision analysis. *Trans. Korean Society of Automotive Engineers* **8, 4,** 177–185.

Kanninen, M. F. and Popelar, C. H. (1985). *Advanced Fracture Mechanics*. Oxford Engineering Science Series 15. London.

Knott, J. F. (1973). *Fundamentals of Fracture Mechanics*. Butterworth Publishers. London.

Malvern, L. E. (1951). The propagation of longitudinal waves of plastic deformation in a bar of material exhibiting a strain-rate effect. *J. Appl. Mech.* **18,** 203–208.

Nakamura, T., Shih, C. F. and Freund, L. B. (1986). Analysis of a dynamically loaded three point bend ductile fracture specimen. *Eng. Frac. Mech.* **25,** 323–339.

Nakamura, T., Shin, C. F. and Freund, L. B. (1985). Elastic-plastic analysis of a dynamically loaded circumferentially notched round bar. *Eng. Frac. Mech.* **22,** 437–452.

Perzyna, P. (1966). *Advances in Applied Mechanics*. Academic Press. New York and London.

Shih, C. F. (1982). Relationship between the J-integral and the crack mouth opening displacement for stationary and extending cracks. *J. Mech. and Phys. of Solids* **29,** 305–326.

Van Elst, H. G. (1984). Assessment of dynamic fracture propagation resistance at instrumented high velocity gasgun impact tests on SENB-Specimens. *ICF* **6, 5,** 3089–3097.

Zehnder, A. T., Rosakis, A. J. and Krishnaswamy, S. (1990). Dynamic measurement of the J-integral in ductile metals: Comparison of experimental and numerical techniques. *Int. J. Frac.*, **42,** 209–230.